Virology 510 (2017) 194–204

Contents lists available at ScienceDirect

Virology

journal homepage: www.elsevier.com/locate/yviro

Differential use of 3'CITEs by the subgenomic RNA of Pea enation mosaic virus 2

Feng Gao, Anne E. Simon*

Department of Cell Biology and Molecular Genetics, University of Maryland, College Park, MD 20742, USA

ARTICLE INFO

Keywords:
Cap-independent translation enhancers
Umbravirus
Pea enation mosaic virus
Subgenomic RNA
Leaky scanning
Translation initiation

ABSTRACT

The genomic RNA (gRNA) of *Pea enation mosaic virus 2* (PEMV2) is the template for p33 and −1 frameshift product p94. The PEMV2 subgenomic RNA (sgRNA) encodes two overlapping ORFs, p26 and p27, which are required for movement and stability of the gRNA. Efficient translation of p33 requires two of three 3' proximal cap-independent translation enhancers (3'CITEs): the kl-TSS, which binds ribosomes and engages in a long-distance interaction with the 5'end; and the adjacent eIF4E-binding PTE. Unlike the gRNA, all three 3'CITEs were required for efficient translation of the sgRNA, which included the ribosome-binding 3'TSS. A hairpin in the 5' proximal coding region of p26/p27 supported translation by the 3'CITEs by engaging in a long-distance RNA:RNA interaction with the kl-TSS. These results strongly suggest that the 5' ends of PEMV2 gRNA and sgRNA connect with the 3'UTR through similar long-distance interactions while having different requirements for 3'CITEs.

1. Introduction

Positive-sense, monopartite RNA viruses that infect eukaryotic hosts encode multiple viral proteins on their single genomic (g)RNA. However, eukaryotic canonical translation is nearly always monocistronic, with translation initiating near the 5' end of the mRNA and then proceeding in a 5' to 3' direction until reaching a termination codon (Aitken and Lorsch, 2012; Jackson et al., 2010). To circumvent this limitation, polycistronic RNA viruses must use one or more non-canonical mechanism to synthesize their proteins, including internal ribosome entry, re-initiation, leaky scanning and translational recoding (Firth and Brierley, 2012; Miras et al., 2017). In addition, with the exception of viruses in the *Potyviridae* and *Secoviridae* that employ a polyprotein expression strategy for gRNA translation (Zaccomer et al., 1995), many RNA viruses produce at least one subgenomic RNA (sgRNA), which repositions downstream ORFs proximal to a 5' end (Firth and Brierley, 2012; Miras et al., 2017). The majority of sgRNAs are 3' co-terminal with the gRNA, although sgRNAs that are 5' co-terminal are associated with some viruses (Gowda et al., 2003; Tatineni et al., 2009; Vives et al., 2002).

Many plant RNA viruses lack 5' caps and 3' poly(A) tails, and efficient translation relies on 3' cap-independent translation enhancers (3'CITEs) (Nicholson and White, 2011; Simon and Miller, 2013). 3'CITEs are located wholly or partially within 3'UTRs and therefore are present in both the gRNA and any 3'co-terminal sgRNAs. Based on their structures, 3'CITE have been placed into several categories including: translation enhancer domain (TED), which were originally discovered in *Satellite tobacco necrosis virus*; Y-shaped structure (YSS), which are found exclusively in tombusviruses; I-shaped structure (ISS), present in a subset of tombusviruses, aureusviruses and carmoviruses; T-shaped structure (TSS), present in several carmoviruses and umbraviruses; Panicum mosaic virus-like translational enhancer (PTE), found in panicoviruses and a subset of aureusviruses, carmoviruses and umbraviruses; and Barley yellow dwarf virus (BYDV)-like element (BTE), found in luteoviruses, dianthoviruses, alphanecroviruses, betanecroviruses and some umbraviruses (Nicholson and White, 2011; Simon and Miller, 2013). 3'CITEs mainly facilitate translation by recruiting translation initiation factor eIF4F, *via* binding to its eIF4E and/or eIF4G subunits, followed by attraction of 40S subunits (Das Sharma et al., 2015; Gazo et al., 2004; Nicholson et al., 2010, 2013; Treder et al., 2008; Wang et al., 2009). In addition, some 3'CITEs can directly bind ribosomes or ribosomal subunits (Das Sharma et al., 2015; Gao et al., 2012, 2014; Stupina et al., 2008). Recruited translation elements are usually delivered to the 5' end of the gRNA *via* a long-distance RNA:RNA interaction between the terminal loop of a hairpin associated with the 3'CITE and accessible sequences in the 5'UTR or nearby coding region (Chattopadhyay et al., 2011; Fabian and White, 2004, 2006; Gao et al., 2012; Nicholson and White, 2008; Nicholson et al., 2010; Simon and Miller, 2013; Wu et al., 2009). 3'CITEs are also assumed to enhance translation of any 3' co-terminal

* Corresponding author.
E-mail address: simona@umd.edu (A.E. Simon).

http://dx.doi.org/10.1016/j.virol.2017.07.021
Received 16 June 2017; Received in revised form 14 July 2017; Accepted 19 July 2017

sgRNAs, and complementary sequences allowing for long-distance interactions between sgRNA 5' regions and 3'CITE hairpins have been predicted and in a few cases validated (Chattopadhyay et al., 2014). However, sgRNA sequences suggested as potential pairing partners for the BTE of *Tobacco necrosis virus D* are not required for efficient translation of viral proteins *in vitro* (Chkuaseli et al., 2015).

While most viruses contain a single 3'CITE, one virulent isolate of *Melon necrotic spot virus* (MNSV-N) contains a second, previously unobserved 3'CITE that was acquired through interfamiliar recombination with a polerovirus and permits infection of otherwise resistant melon varieties (Miras et al., 2014). Another virus with multiple 3'CITEs is the umbravirus *Pea enation mosaic virus 2* (PEMV2), which has three 3'CITEs in its unusually long (703 nt) 3'UTR (Gao et al., 2014). These 3'CITEs are: (1) the kissing-loop T-shaped structure (kl-TSS), which binds 80S ribosomes and 40S and 60S ribosomal subunits and engages in a long-distance RNA:RNA interaction with a 5' end hairpin (5H2) in the coding region of the 5' proximal ORF (Gao et al., 2012); (2) the PTE, which is located just downstream of the kl-TSS and binds to eIF4E (Wang et al., 2009); and (3) the 3'TSS, which is also capable of binding to 80S ribosomes and 60S ribosomal subunits and is similar to the well-studied TSS of carmovirus *Turnip crinkle virus* (Gao et al., 2014; Stupina et al., 2008) (Fig. 1B). Only the kl-TSS and PTE were required for translation of full-length PEMV2 gRNA in wheat germ extracts (WGE) (Du et al., 2017), or reporter constructs containing the entire 3'UTR of PEMV2 (Gao et al., 2014) and thus the functional role of the 3'TSS is unknown.

The umbravirus genus within the *Tombusviridae* is unusual in that its member viruses do not code for a coat protein (CP) (Adams et al., 2015). While fully capable of replicating in plant cells and establishing a systemic infection within a host plant, umbraviruses require a helper virus (commonly a polerovirus or enamovirus) for encapsidation and aphid transmission. The helper virus for PEMV2, the enamovirus PEMV1, is incapable of systemic movement in the absence of the PEMV2-encoded movement proteins (MP). PEMV2, whose positive-sense genome (4252 nt) contains no 5'cap or 3' poly(A) tail (Demler et al., 1993), has 4 ORFs that encode: (1) p33, a protein likely associated with replication (when compared with similar proteins in other tombusvirids); (2) p94, the RNA-dependent RNA polymerase (RdRp), whose expression requires −1 ribosomal frameshifting to bypass the termination codon at the end of the p33 ORF (Demler et al., 1993; Gao and Simon, 2016); (3) p26; and (4) p27, whose ORF nearly completely overlaps with the p26 ORF (Fig. 1A). p26 does not share sequence similarity with any non-umbravirus proteins and serves as both a long-distance MP and as a stabilizing protein, functionally substituting for the TMV CP in long-distance movement of TMV gRNA (Ryabov et al., 2001). In addition, the p26 orthologue of umbravirus *Groundnut rosette virus* (GRV) redistributes nucleolar protein fibrillarin to the cytoplasm, which facilitates long-distance movement through the phloem (Kim et al., 2007a, b). As a stabilizing protein, p26 forms ribonucleoprotein particles with viral RNA, likely protecting it from the host RNA silencing machinery and degradation by other cellular nucleases (Taliansky et al., 2003). The GRV p27 orthologue is a cell-to-cell MP, which can functionally replace the MP of unrelated *Potato virus X* and *Cucumber mosaic virus* (Ryabov et al., 1998, 1999). Whereas p33 and p94 are related to their counterparts in carmoviruses, the origin of p26 and p27 is more obscure. p27 shares 26% amino acid identity and 50% nucleotide sequence identity with a putative MP encoded by the 5' proximal ORF of unclassified *Japanese holly fern mottle virus* (JHFMoV) RNA2 (Valverde and Sabanadzovic, 2009), and thus may have been acquired by a recombination event. However, no overlapping ORF corresponding to a p26-type protein in JHFMoV is discernable.

p33 and p94 are translated from the PEMV2 gRNA, and p26 and p27 are translated from an as yet uncharacterized sgRNA (Fig. 1A). The recent finding that only two of the three PEMV2 3'CITEs (the kl-TSS and PTE) are necessary for efficient translation of the gRNA (Du et al., 2017) suggested that the 3'TSS may function in translation of the sgRNA. In the current study, we investigated this possibility by mapping the PEMV2 sgRNA transcription start site, which allowed for translation of full-length sgRNA transcripts in WGE and for the generation of reporter constructs to assay for translation *in vivo*. We determined that efficient translation *in vitro* and *in vivo* required the PTE and a long-distance RNA:RNA interaction between the kl-TSS and an sgRNA coding region hairpin. In addition, we determined that, unlike translation of the gRNA, the 3'TSS is as important as the PTE for translation of the sgRNA in WGE. Furthermore, all three 3'CITEs enhanced translation of reporter constructs carrying sgRNA 5' and 3' sequences *in vivo*. These data suggest that PEMV2 gRNA and sgRNA have different translation mechanisms, which could be an effective strategy for fine-tuning viral gene expression at various stages of the viral infection cycle.

2. Results

2.1. Mapping the transcription start site of PEMV2 sgRNA

As previously reported (Gao and Simon, 2016), inoculation of Arabidopsis protoplasts with *in vitro*-transcribed PEMV2 gRNA results in the accumulation of gRNA and a putative sgRNA of approximately 1.5 kb (see Fig. 1E, lane 2). To map the precise transcription start site of the putative sgRNA, primer extension reactions were performed using total RNA isolated from PEMV2-infected protoplasts at 24 h post-inoculation (hpi) and a primer complementary to positions 2845–2869. A sequence ladder was generated using the same primer and *in vitro*-transcribed gRNA as template. PEMV2 containing a GDD mutation in the RdRp active site that eliminates enzyme activity was used as a negative control.

As shown in Fig. 1C, reverse transcription reactions using wt PEMV2 generated a strong-stop product corresponding to a guanylate at position 2772 (G2772), which would correspond to a 3' co-terminal sgRNA of 1481 nt. The PEMV2 sequence beginning at position 2772 is 5'-GGGAAAUAU, which is similar to the sequence at the 5' end of the gRNA (5'GGGUAUUUA). Genomic RNA and sgRNA of related carmoviruses are known to begin with a "Carmovirus Consensus Sequence" or CCS, which consists of one to three guanylates (usually two or three) followed by a short stretch of A/U residues (Guan et al., 2000). Umbravirus gRNAs, with the exception of *Carrot mottle virus* (CMoV), *Tobacco bushy top virus* (TBTV) and *Carrot mottle mimic virus* (CMoMV), also have a canonical CCS at their 5' ends. The presence of a CCS at position 2772 in PEMV2 supports the designation of G2772 as the 5' terminus of the sgRNA. Examination of other umbraviruses revealed that, with the exception of CMoV and CMoMV, each has a CCS in an equivalent position upstream of their p26-corresponding ORFs (Fig. 1D). The PEMV2 sgRNA has a short 9-nt 5'UTR followed by p26 and p27 overlapping ORFs, with 16 nt separating the two initiation codons (AUG^{26} and AUG^{27}). A 16-nt spacer between AUG^{26} and AUG^{27} is also present in other umbraviruses with the exception of CMoV and CMoMV, where the spacer is slightly longer.

To determine the importance of p26 and p27 for PEMV2 accumulation in protoplasts, gRNA transcripts containing point mutations in AUG^{26} and/or AUG^{27} (AUG to CAG) were inoculated onto protoplasts and gRNA levels were examined by Northern blots at 24 hpi. Altering AUG^{26} (m1) reduced gRNA accumulation by over 4-fold (Fig. 1E). In contrast, mutations in AUG^{27} (m2) resulted in a 1.7-fold increase in gRNA levels. Combining both mutations (m1 + m2) reduced gRNA levels to a similar extent as m1 alone. This result indicates that p26, but not p27, is important for robust PEMV2 gRNA accumulation in protoplasts. Since no movement is associated with protoplast infection, it is likely the stabilizing property of p26 that is required for efficient gRNA accumulation in single cells.

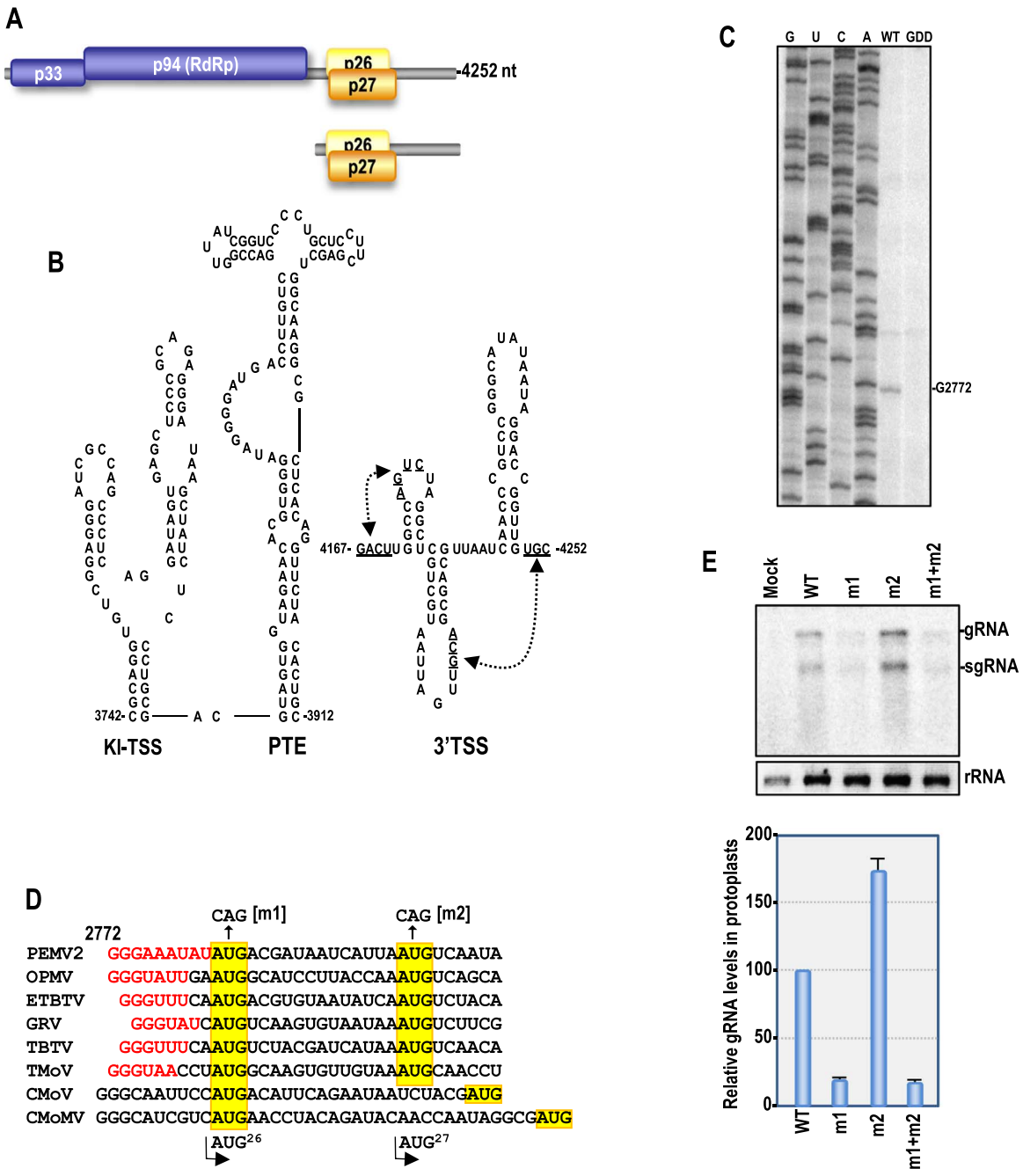

Fig. 1. Mapping the transcription start site of PEMV2 sgRNA and the biological importance of its encoded products. (A) Genome organization of PEMV2. p33 and −1 ribosomal frameshifting product p94 are expressed from the gRNA. p26 and p27 are expressed from overlapping ORFs on the sgRNA. (B) Secondary structures of the three PEMV2 3'CITEs located in the 3'UTRs of the gRNA and sgRNA. Double arrows represent known tertiary interactions between underlined residues. (C) Primer extension assay mapping the transcription start site of PEMV2 sgRNA using total RNA from Arabidopsis protoplasts transfected with wt PEMV2 gRNA (WT) or replication-incompetent mutant GDD. G, U, C, A, sequencing ladder lanes. Position of the primer extension product at G2772 is indicated. (D) Alignment of PEMV2 AUG^{26} and the equivalent initiation codons from other umbraviruses. AUG^{26} and AUG^{27} are highlighted in yellow. Putative CCS sequences are in red. m1 and m2 mutations are shown. *Opium poppy mosaic virus* (OPMV) (EU151723), *Ethiopian tobacco bushy top virus* (ETBTV) (NC_024808), *Groundnut rosette virus* (GRV) (NC_003603.1), *Tobacco bushy top virus* (TBTV) (KM_067277.1), *Tobacco mottle virus* (TMoV), (AY007231), *Carrot mottle virus* (CMoV) (NC_011515.1) and *Carrot mottle mimic* virus (CMoMV) (NC_001726.1). (E) Upper panel, Northern blot analysis of PEMV2 gRNA and sgRNA accumulation in Arabidopsis protoplasts transfected with wt or mutant viruses at 24 hpi. Positions of the gRNA and sgRNA are indicated. 28S ribosomal RNA (rRNA) served as the loading control. Lower panel, Quantification of PEMV2 gRNA levels in protoplasts. Mean values and standard error were calculated from at least three independent experiments.

2.2. p26 and p27 translation initiation is competitive

Translation of wild-type (wt) PEMV2 sgRNA in WGE resulted in two major products that migrated in SDS-PAGE gels at size markers positions of 25 kDa and 28 kDa (Fig. 2A). Unexpectedly, alteration of AUG^{26} to CAG, which is not known to serve as a non-canonical start codon (Hecht et al., 2017), eliminated detection of the slower-migrating product (m1; Fig. 2A, left panel). Converting the p26 stop codon (and nearby downstream stop codon) to sense codons (UGA -9 nt- UAG to AGA -9 nt- GAA) also resulted in loss of the slower-migrating product and generation of an extension product (p26 UGAm; Fig. 2B, left panel). This indicates that the slower migrating product corresponds to p26. Similarly, the amount of the faster migrating product was significantly reduced when AUG^{27} was mutated (m2; Fig. 2A, right panel). In addition, changing the p27 stop codon to sense codon GGA caused the lower band to shift upward and co-migrate with p26 (p27

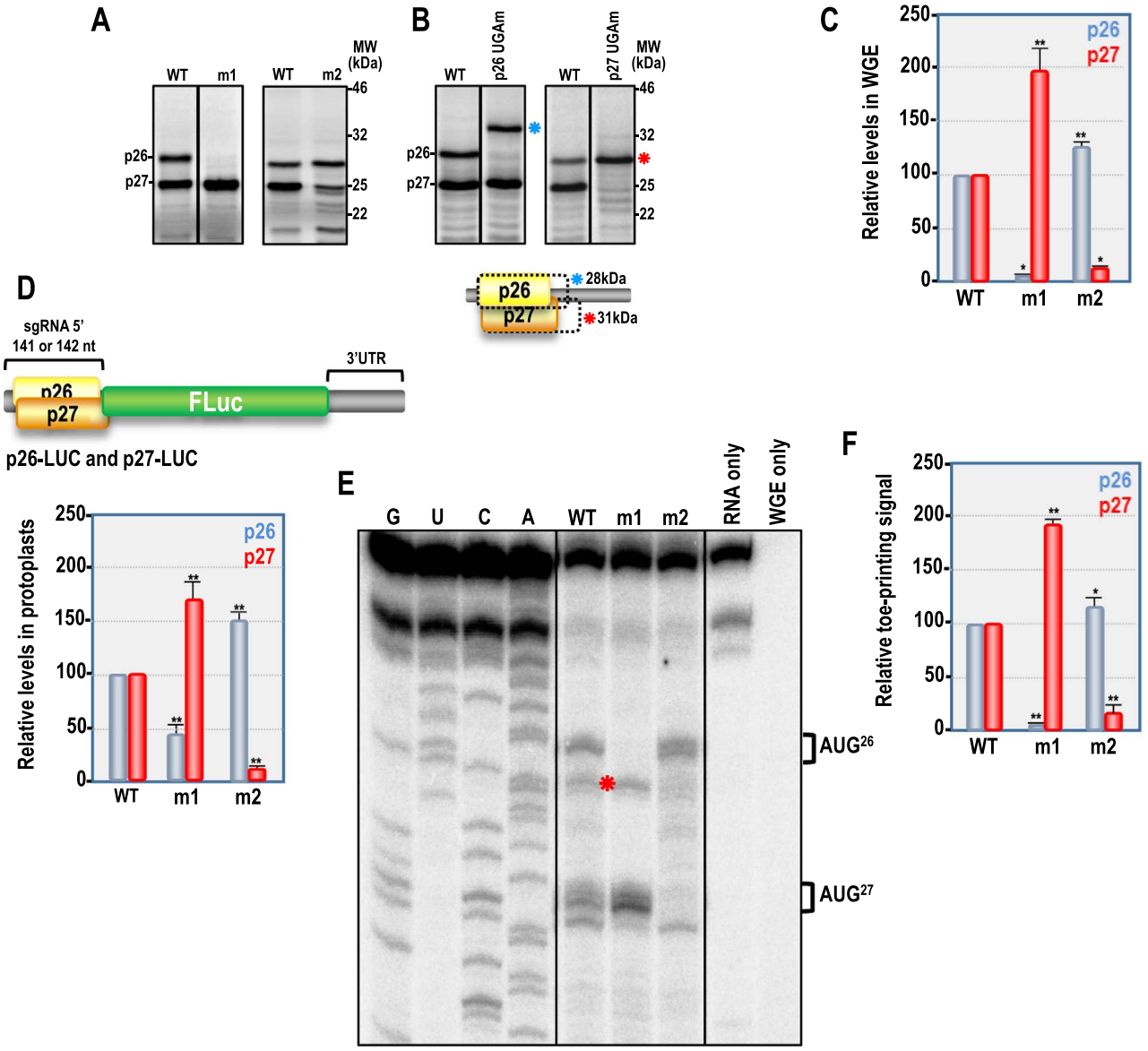

Fig. 2. Translation of full-length sgRNA in WGE and luciferase reporter constructs in Arabidopsis protoplasts. (A) *In vitro* translation of sgRNA in WGE. Bands corresponding to p26 and p27 are labeled. m1 and m2 alternations are described in Fig. 1D. Vertical lines denote removal of lanes from the images shown. MW, protein molecular weight markers. (B) WGE assay showing products generated when termination codons were mutated. p26 UGAm (UGA -9 nt- UAG to AGA -9 nt- GAA) should generate a product of 28 kDa and p27 UGAm (UGA to GGA) should generate a product of 31 kDa. Asterisks denote locations of the extension products. (C) Quantification of the relative levels of p26 and p27 from A. Mean values and standard error were calculated from at least three independent experiments. Unpaired *t*- test was used to analyze the statistical significance. *, $P \leq 0.05$; **, $P \leq 0.01$. (D) Relative luciferase activity in protoplasts transfected with transcripts of p26-LUC and p27-LUC. Renilla luciferase transcripts were co-transfected to serve as an internal control. Mean values and standard error were calculated from at least three independent experiments. (E) Ribosome toeprinting of sgRNA in WGE. Ribosomes were stalled at AUG^{26} and AUG^{27} by addition of CHX at the beginning of the translation assay and primer extension was performed to determine the location of stalled ribosomes. The toeprints corresponding to stalled ribosomes at AUG^{26} and AUG^{27} are labeled. Asterisk denotes additional AUG^{27} toeprint that may represent improper fixing of the sgRNA in the mRNA-binding cleft of the 40S subunit, allowing for further extension by the reverse transcriptase (Battiste et al., 2000; Pisareva et al., 2008). G, U, C, A are ladder lanes. RNA transcripts (RNA only) or the translation reaction in the absence of added RNA template (WGE only) served as negative controls. (F) Quantification of the intensity of toeprints shown in E. Mean values and standard error were calculated from at least three independent experiments.

UGAm; Fig. 2B, right panel). These results indicate that both p26 and p27 migrate aberrantly on SDS gels. Translation of p27 was 1.7-fold more efficient than p26 in WGE, after accounting for the number of ^{35}S methionines incorporated.

Increased translation of p27 in the absence of AUG^{26} would be expected if a ribosome leaky scanning mechanism is used for translation initiation at the closely spaced AUG^{26} and AUG^{27} (Firth and Brierley, 2012; Kozak, 1999; Miras et al., 2017; Thiebeauld et al., 2007). In leaky scanning, ribosomes occasionally bypass one or more initiation codons in a weak context and initiate translation downstream at an AUG in a stronger context. However, both AUG^{26} and AUG^{27} are in a poor context (uridylates at −3 and no guanylate at + 1) (Kozak, 1999) and translation of p26 was also 27% higher in the absence of downstream p27 translation (Fig. 2C). To determine whether similar results are obtained *in vivo*, luciferase reporter constructs were generated in which the sgRNA 5'UTR and the N-terminal 49 or 44 codons of p26 or p27 ORFs, respectively, were fused in frame with firefly luciferase ORF (FLuc) followed by the complete 3'UTR of PEMV2 (designated p26-LUC and p27-LUC). p26-LUC and p27-LUC differ by a single nucleotide in the junction region between the sgRNA 5' sequence and luciferase sequence. Arabidopsis protoplasts were transfected with transcripts of p26-LUC or p27-LUC along with transcripts of Renilla luciferase as an internal control. Elimination of AUG^{26} in p27-LUC increased translation of p27 by 1.7-fold, identical to

what was found for full-length sgRNA assayed in WGE (m1; Fig. 2D). In addition, translation of p26 was enhanced 1.5-fold when AUG^{27} was mutated in p26-LUC m2 (m2; Fig. 2D). Taken together, these results suggest that translation initiating from AUG^{26} and AUG^{27} is competitive both *in vitro* and *in vivo* and may not involve a canonical leaky-scanning mechanism.

Ribosome toeprinting experiments were conducted to investigate whether the enhanced translation that occurs when only one ORF is translated was due to an increase in ribosomes accessing the initiation codon. This assay, which was conducted in WGE in the presence of cycloheximide (CHX), examines ribosome occupancy at the initiation codon since CHX interferes with ribosome translocation. Two major toeprints were detected that correspond to ribosomes stalled at AUG^{26} and AUG^{27} (Fig. 2E). In the absence of AUG^{26}, the toe print corresponding to AUG^{27} was enhanced by nearly 2-fold whereas the AUG^{26} toeprint was enhanced by 21% in the absence of AUG^{27}. These results correlate well with the WGE translation results, strongly suggesting that differences in translation of p26 and p27 in WGE using wt and mutant transcripts reflect differences in translation initiation.

2.3. Translation of p26 and p27 is dependent on all three 3'CITEs

Robust translation of full-length gRNA in WGE only requires the PTE and the kl-TSS, *i.e.,* removing the 3'TSS had no effect on full-length gRNA translation in WGE (Du et al., 2017). In addition, only the kl-TSS and PTE were required to significantly enhance translation of luciferase reporter constructs containing the PEMV2 full-length 3'UTR and the 5' end 89-nt, which includes hairpin 5H2, the hairpin that participates in the long-distance interaction with the kl-TSS (Gao et al., 2012, 2014). However, the 3'TSS was important for accumulation of PEMV2 gRNA in protoplasts (Gao et al., 2014). In addition, when reporter constructs' 3'UTR contained a deletion that removed the kl-TSS and PTE and placed the 3'TSS proximal to the luciferase termination codon, the 3'TSS enhanced translation in conjunction with a nearby hairpin that base-pairs with 5' hairpin 5H2. These studies together suggested that while the 3'TSS is an important element for viral gRNA accumulation and is capable of enhancing translation in modified reporter constructs, its role in translation in the infection cycle of the PEMV gRNA was unsolved.

Finding that the 3'TSS was dispensable for translation of the gRNA in WGE and gRNA reporter constructs with full-length 3'UTR *in vivo* naturally led to questions about its function. To determine whether the 3'TSS might be important for translation of the sgRNA, the kl-TSS, PTE and 3'TSS were deleted either individually or in combination, and otherwise full-length sgRNA transcripts assayed for p26 and p27 translation over time in WGE. Deletion of the PTE alone (ΔP) reduced synthesis of p26 and p27 by 32% and 36% respectively after 45 min, and deletion of the kl-TSS alone (ΔK) reduced translation by 48% and 56%, respectively (Fig. 3A and B). Deletion of the 3'TSS alone (ΔT) decreased translation of p26 by 32% and p27 by 36%, equivalent to the reductions obtained for ΔP. Deletion of the kl-TSS together with either the PTE or 3'TSS in reduced levels of p26 and p27 to amounts found when the entire 3'UTR was deleted (50% and 70%, respectively; Fig. 3A-D). Individual deletions of the three 3'CITE in p26-LUC and p27-LUC also reduced luciferase activity in protoplasts, with ΔK reducing activity ~2-fold more than ΔP or ΔT (Fig. 3E). For both WGE and protoplast assays, 3'CITE deletions affected p27 translation (or luciferase translation from AUG^{27}) more than p26 (or luciferase translation from AUG^{26}). These results strongly suggest that, unlike translation of the gRNA, all three 3'CITEs are important for efficient translation of the sgRNA.

2.4. The PTE inhibits translation of sgRNA in trans

We previously demonstrated that the PTE inhibits translation of the gRNA *in trans* due to sequestration of limiting quantities of eIF4F (Du et al., 2017). To determine if the PTE also inhibits translation of the sgRNA *in trans*, 10-fold molar excess of PTE was included with sgRNA transcripts in the WGE assay. Addition of wt PTE caused a 37% and 41% reduction in synthesis of p26 and p27, respectively. This result was comparable to the ~40% reduction in translation of the gRNA using similar WGE assay conditions (Du et al., 2017). In contrast, addition of a PTE mutant incapable of binding to eIF4E (PTEm2) (Du et al., 2017) had no detrimental effect on translation (Fig. 4). When the PTE was added *in trans* with ΔKΔPΔT (*i.e.,* no PTE is present in the sgRNA template *in cis*), translation of p26 and p27 was reduced by 2.6-fold and 3-fold, respectively. This reduction was notably less than the 5-fold reduction found for ΔKΔPΔT gRNA (Du et al., 2017). These results suggest that 3'CITE-independent translation of the sgRNA is dependent on eIF4E/eIF4G, but to a lesser extent than the gRNA.

2.5. The kl-TSS and the PTE, but not the 3'TSS, enhance ribosome recruitment at AUG^{26} and AUG^{27}

To determine if translation enhancement by 3'CITEs is due to more efficient recruitment of ribosomes at AUG^{26} and AUG^{27}, sgRNA transcripts containing 3'CITE deletions were subjected to ribosome toeprinting in the presence of CHX. The absence of the 3'UTR (Δ3'UTR) reduced ribosome toeprints at AUG^{26} and AUG^{27} to 23% and 16% of wt, respectively (Fig. 5B), which is ~2-fold lower than the corresponding reduction in translation efficiency (Fig. 3A and B). Similar reductions in ribosome toeprints were observed for ΔKΔPΔT. ΔK by itself reduced ribosome toeprints at AUG^{26} and AUG^{27} by 34% and 52% respectively, whereas ΔP reduced toeprints by 48% and 61%, respectively. These results suggest that the kl-TSS and PTE enhance translation by facilitating ribosome recruitment at AUG^{26} and AUG^{27}. In contrast, ΔT, which reduced translation by a similar amount as ΔP, did not significantly reduce ribosome toeprints (Fig. 5B). This suggests that the 3'TSS enhances translation by a mechanism that takes place after ribosome positioning at the initiation codon.

2.6. Efficient sgRNA translation requires a long-distance RNA-RNA interaction between the kl-TSS and a 5' coding region hairpin

The terminal loop of the 5' side hairpin of the kl-TSS is known to participate in a long-distance interaction with a 5' proximal, p33 coding-region hairpin (5H2) (Fig. 6A), which does not interfere with ribosomes binding to the kl-TSS (Gao et al., 2013, 2012). To determine if a hairpin capable of interacting with the kl-TSS is similarly positioned near the 5' end of the sgRNA, selective 2' OH acylation analyzed by primer extension (SHAPE) was used to examine the secondary structure of the 5' region of full-length sgRNA transcripts synthesized *in vitro*. The flexibility of each nucleotide was monitored by its reactivity to modification by NMIA, and data were quantified using SAFA software (Das et al., 2005). As shown in Fig. 6B, nucleotides are labeled red for high reactivity, green for moderate reactivity, and black for low reactivity. The sgRNA 5' 57 residues were mainly flexible, suggesting that limited structure exists at the 5' end of the sgRNA. A short hairpin (sgH1) was predicted starting at position 58 (relative to the 5' end of the sgRNA), placing it within the coding regions of p26/p27. The terminal loop contains the sequence 5'-CUGGC, which is complementary to the kl-TSS 5' side hairpin loop sequence (5'-GCCAG) (Fig. 6B). To validate the structure and importance of sgH1, 2-nt alterations were introduced on both sides of the stem (m3 and m4) that together (m3 + m4) should be compensatory and reform the stem (Fig. 6B). Translation of wt and mutant sgRNA in WGE revealed that m3 and m4 reduced translation of p26 by ~25% and p27 by ~50%. m3 + m4 restored translation of p26 to near wt levels and p27 to 80% of wt (Fig. 6C). This supports the existence and importance of the sgH1 stem for translation in WGE.

To determine whether the proposed long-distance RNA:RNA interaction between the sgH1 loop and the kl-TSS is important for

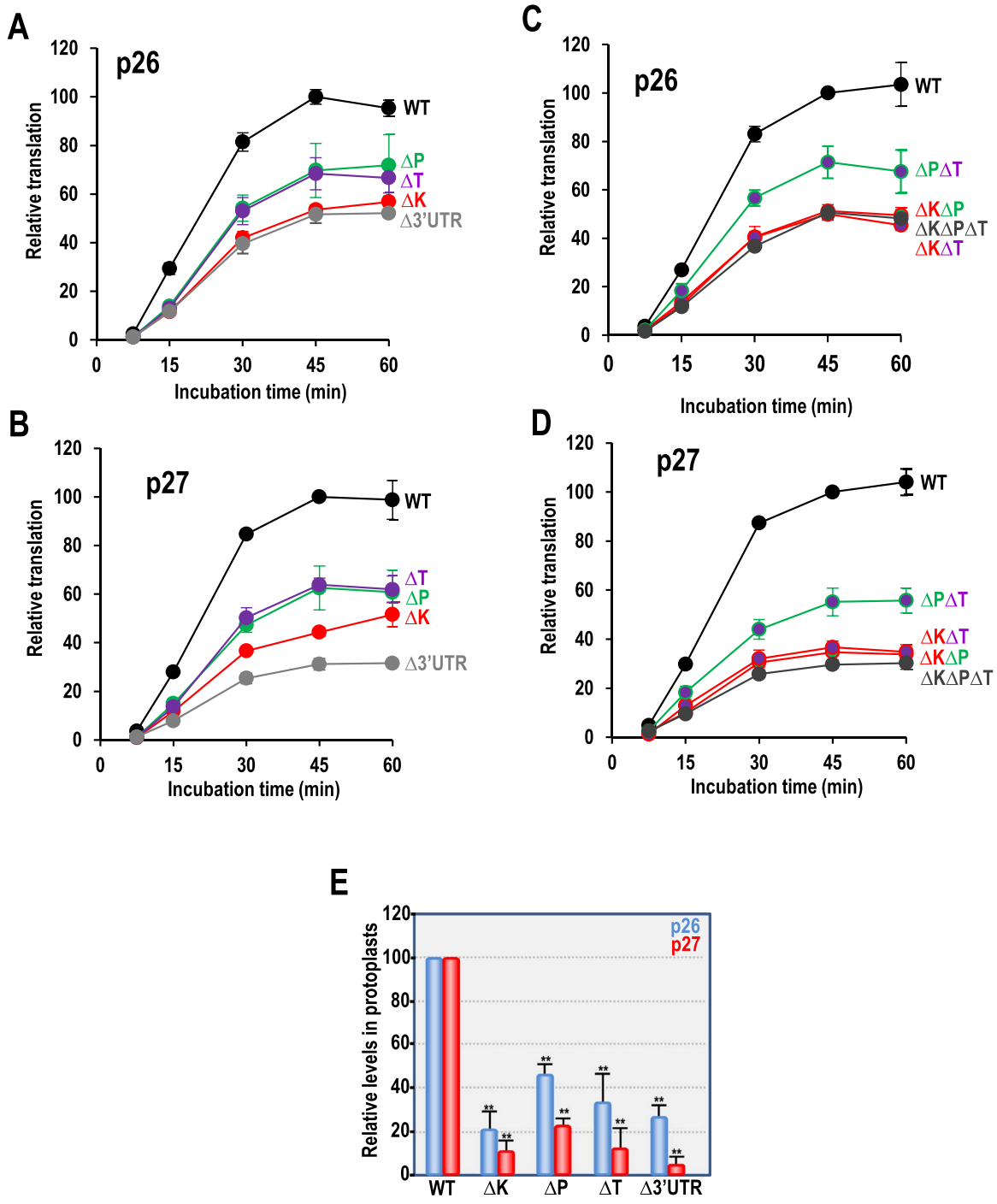

Fig. 3. Contribution of 3'CITEs to translation of sgRNA in WGE. (A-D) sgRNA with single or multiple deletions of 3'CITEs were translated in WGE and p26 (A, C) and p27 (B and D) levels were monitored at various time points. ΔK, deletion of the kl-TSS; ΔP, deletion of the PTE; ΔT, deletion of the 3'TSS; Δ3'UTR, deletion of the 3'UTR. Levels of p26 and p27 were normalized to levels obtained using wt sgRNA at 45 min, which was set to 100. Standard error for each time point was calculated from at least three independent experiments. (E) Transcripts of p26-LUC and p27-LUC containing single 3'CITE deletions were assayed in Arabidopsis protoplasts and luciferase activity measured after 18 h. One-way ANOVA was used to analyze the statistical significance. **, P ≤ 0.01. Mean values and standard error were calculated from at least three independent experiments.

translation, loop sequences were altered in sgH1 (m5) and the kl-TSS (m6) and translation assayed in WGE (Fig. 6B). m5 produced 32% less p26 ($p < 0.05$) and 52% less p27 ($p < 0.01$), whereas m6 reduced translation of p26 by only 21% and p27 by 38% ($p < 0.01$) (Fig. 6C). m5 + m6 restored translation of p26 to 88% of wt and p27 to 75% (Fig. 6C). The same mutations were also introduced into p26-LUC and p27-LUC for translation in protoplasts. Both m5 and m6 reduced luciferase activity by nearly 6-fold in protoplasts, whereas compensatory mutations m5 + m6 restored luciferase activity to nearly 60% of wt (Fig. 6D). Altogether, these results support a long-distance RNA:RNA interaction between sgH1 and the kl-TSS, which is important for efficient translation of the sgRNA *in vivo*.

3. Discussion

Plant viruses in the *Tombusviridae* and *Luteoviridae* lack 5' caps and 3' poly(A) tails and thus require non-canonical mechanisms to attract ribosomes to their translation initiation codons. Since egress of plant viruses requires living cells, they must translate their genomes in competition with continued translation of cellular mRNAs. Most viruses

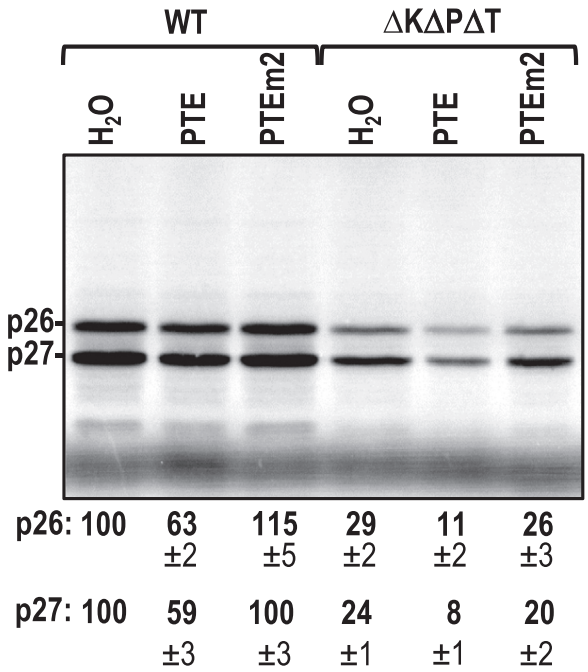

Fig. 4. Addition of PTE fragments *in trans* inhibits translation of wt and ΔKΔPΔT sgRNAs. WT sgRNA or ΔKΔPΔT sgRNA were translated in the presence of a 10-fold molar access of the PTE or PTEm2 (a PTE mutant incapable of binding to eIF4E) in WGE. Mean values and standard error were calculated from at least three independent experiments.

in these families have short 5'UTRs, which necessitates placement of ribosome-attracting elements in or near their 3'UTRs, with long-distance RNA:RNA interactions connecting these elements with the 5' end of the genome (Miras et al., 2017; Simon and Miller, 2013). The 3' location of translation elements would also enable tombusvirid and luteovirid gRNA and any 3' co-terminal sgRNA to share the same 3'CITE-dependent translation mechanism. For that reason, the few reports that include translation of sgRNAs mainly emphasize the presence and location of any 5'/3' interacting sequences (Chattopadhyay et al., 2014; Fabian and White, 2004; Shen et al., 2006) and not possible differences between translation requirements of gRNA and sgRNA templates.

PEMV2 is unique (so far) in possessing three 3'CITEs in its 3'UTR. Among them, only the kl-TSS and the adjacent PTE contribute to translation of the full-length gRNA in WGE (Du et al., 2017), as well as translation of reporter constructs with 5' gRNA sequences and the full-length 3'UTR in protoplasts (Gao et al., 2014). The 3'TSS, while not important for gRNA translation in these assays, is important for accumulation of the gRNA in protoplasts (Gao et al., 2014). In addition, the 3'TSS can enhance translation of luciferase reporter constructs missing the kl-TSS and PTE, with the long-distance interaction provided by a 3'TSS-proximal hairpin (Gao et al., 2014). While these studies led to identification of three 3'CITEs, they left unresolved the purpose of the 3'TSS in accumulation of full-length PEMV2 in natural infections.

3.1. sgRNA CCS are within a stem loop conserved in umbraviruses

The 3'TSS of PEMV2 and TCV consist of three hairpins and two pseudoknots and similar configurations of known or putative hairpins and pseudoknots are found in comparable locations relative to the 3' terminus of umbraviruses CMoV, TBTV, and *Opium poppy mosaic virus*; and carmoviruses TCV, *Cardamine chlorotic fleck virus*, and *Japanese iris necrosis ringspot virus* (Gao et al., 2014; McCormack et al., 2008). The TCV TSS was inactive in full-length gRNA assayed in WGE (Simon, unpublished) and in reporter constructs assayed in WGE (Stupina et al., 2008). However, the TCV TSS strongly enhanced translation of gRNA reporter constructs in protoplasts (Stupina et al., 2008). In contrast, the PEMV2 3'TSS did not enhance translation of similar gRNA reporter constructs in protoplasts (Gao et al., 2014). To address the possibility that the PEMV2 3'TSS might function to enhance translation of the sgRNA, we needed to map the 5' end of the sgRNA (Fig. 1). The 5' extension product indicated that PEMV2 sgRNA begins with a CCS, similar to the CCS at the 5' end of the PEMV2 gRNA. The presence of CCS at the 5' ends of PEMV2 gRNA and sgRNA is similar to what is found for related carmoviruses (Guan et al., 2000). CCS-complementary sequences are likely promoters for the RdRp, and could be used to generate sgRNA either following premature termination of minus-strand synthesis or by internal initiation of transcription using the minus-strand gRNA as template (Sztuba-Solinska et al., 2011). sgRNA2 of TCV (encoding the CP) is synthesized following premature termination of minus-strand synthesis, with the CCS just downstream (in the plus-strand) from a stable hairpin (Wang and Simon, 1997; Wu et al., 2010). All umbraviruses contain similarly positioned stable hairpins, which differ from carmoviruses in that the stems appear to incorporate the three CCS guanylates (Fig. 7). Also

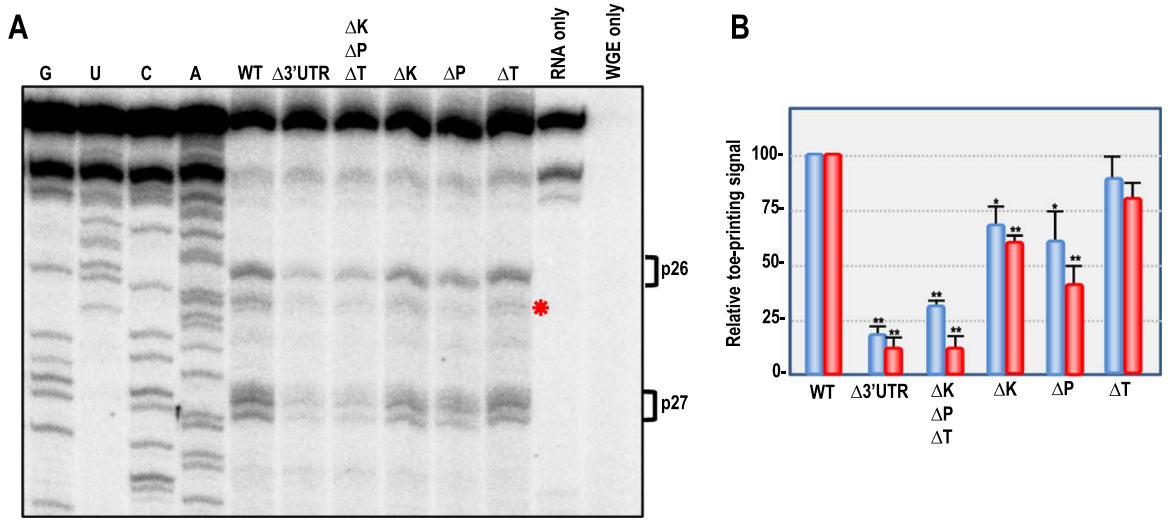

Fig. 5. Ribosome toeprinting of wt and mutant sgRNAs with deletion of single 3'CITEs in WGE. (A) Toeprints corresponding to stalled ribosomes on AUG^{26} and AUG^{27} are labeled. The asterisk denotes additional toeprint described in legend to Fig. 2E. G, U, C, A are ladder lanes. RNA only and WGE only lanes are described in Fig. 2E. (B) Quantification of the intensity of toeprints shown in A. One-way ANOVA was used to analyze the statistical significance. *, $P \leq 0.05$; **, $P \leq 0.01$. Mean values and standard error were calculated from at least three independent experiments.

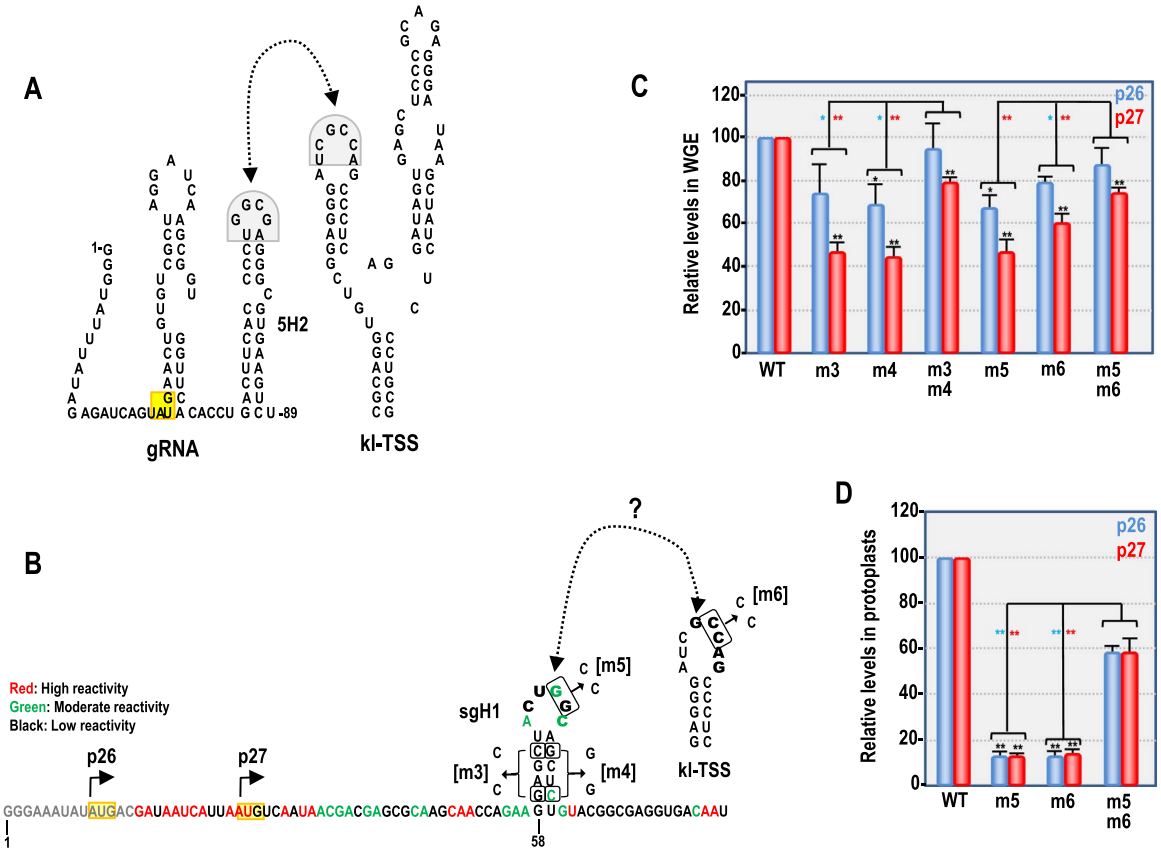

Fig. 6. Long-distance RNA:RNA interaction between the kl-TSS and sgH1 is required for efficient translation of sgRNA in WGE and Arabidopsis protoplasts. (A) Long-distance interaction between the kl-TSS 5' hairpin and p33 coding-region hairpin 5H2. Complementary sequences are shaded gray. p33 initiation codon is shaded yellow. (B) sgRNA 5' end secondary structure determined by SHAPE. Residues are colored red for high reactivity to NMIA, green for moderate reactivity, and black for low reactivity. Residues with unavailable SHAPE data are colored gray. Double arrows represent the proposed long-distance RNA:RNA interaction between the kl-TSS and sgH1. Complementary sequences are in bold. Base substitutions that disrupt the sgH1 stem (m3 and m4) or the long distance RNA:RNA interaction (m5 and m6) are shown. (C) Translation of wt and mutant sgRNAs in WGE. (D) Relative luciferase activity in protoplasts transfected with wt or mutant p26-LUC or p27-LUC. Significant differences with wt are shown with black asterisks. Significant differences between single mutations and the compensatory mutations are shown with colored asterisks (blue, p26; red, p27). One-way ANOVA was used to analyze statistical significance. *, $P \leq 0.05$; **, $P \leq 0.01$. Mean values and standard error were calculated from at least three independent experiments.

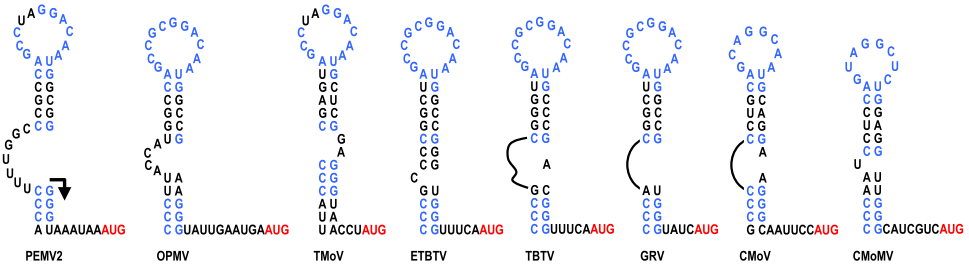

Fig. 7. Conservation of putative structures in the vicinity of the umbravirus CCS. Putative structures immediately upstream of umbravirus CCS were predicted by mfold. Conserved sequences in the terminal loop and the lower stem are colored blue. AUG^{26} is in red. Arrow denotes transcription start site of PEMV2 sgRNA.

unlike carmoviruses, there is strong conservation of the hairpins' terminal loop sequences. Whether the mechanism of sgRNA synthesis resembles that of related carmoviruses is presently under investigation.

The sgRNA hairpin (sgH1) whose terminal loop interacts with the kl-TSS is located within the p26 and p27 coding regions (Fig. 6). Interestingly, the distance from the base of sgH1 to AUG^{26} (45 nt) is similar to the distance from the base of 5H2 (the gRNA hairpin that interacts with the kl-TSS) to the p33 initiation codon (36 nt). Location of hairpins involved in long-distance interactions in the coding region of gRNA and sgRNA can also be found for some carmoviruses (Chattopadhyay et al., 2014, 2011; Simon and Miller, 2013), which differs from tombusviruses, luteoviruses and necroviruses where the interacting sequence is in their longer 5'UTRs (Simon and Miller, 2013). The location of the interacting hairpin either upstream or downstream of the initiation codon may not be consequential as ribosomes are apparently recruited to the 5' end followed by scanning to the appropriate initiation codon (Guo et al., 2001; Rakotondrafara et al., 2006; Sarawaneeyaruk et al., 2009).

3.2. Translation of the sgRNA uses all three 3'CITES

Deletion of any of the 3'CITEs reduced translation of full-length sgRNA *in vitro* and reporter constructs with sgRNA 5' and 3' sequences *in vivo* (Fig. 3A, B and E). Deletion of either the PTE or the 3'TSS reduced synthesis of p26 and p27 by similar amounts (~32% and 36% respectively), with deletion of the kl-TSS reducing translation an additional 35% (Fig. 3). In contrast, loss of the 3'TSS had no discernable effect on translation of full-length gRNA in WGE (Du

et al., 2017) or gRNA reporter constructs with full-length 3'UTRs *in vivo* (Gao et al., 2014). This strongly suggests that, unlike the gRNA, the kl-TSS, PTE, and 3'TSS all contribute to translation of the sgRNA. Since p26 is critical for viral fitness (Fig. 1E), this finding provides an explanation for why the 3'TSS is important for gRNA accumulation in protoplasts (Gao et al., 2014). Curiously, similar losses in translational efficiency by deletion of the 3'TSS and PTE did not correspond to similar reductions in ribosomes occupying AUG^{26} and AUG^{27} in the presence of CHX (Fig. 5). Reduction in p26 and p27 levels in the absence of the kl-TSS or PTE correlated with reduced ribosome occupancy of the initiation codons (Fig. 5), as was previously found for similar deletions in the gRNA (Du et al., 2017). However, lack of the 3'TSS did not significantly reduce ribosome toeprints at either initiation codon. Since ribosome toeprints only measure ribosome occupancy in the pioneer round of translation, it is possible that the 3'TSS facilitates ribosome recruitment during steady-state translation. Alternatively, the 3'TSS may enhance sgRNA translation during an event downstream of ribosome occupancy of the initiation codon.

Translation of the sgRNA also differed from the gRNA in how it was affected by having a PTE in the 3'UTR when the kl-TSS was deleted. Without a long-distance interaction connecting the 3'UTR with the 5' end of the gRNA, the presence of the PTE *in cis* in the gRNA caused an additional 3-fold reduction in translation *in vitro* when compared with levels produced by ΔKΔPΔT or Δ3'UTR (Du et al., 2017). Inhibition of translation by the PTE *in cis* was due to sequestration of limiting quantities of eIF4F, which is required for 3'CITE-independent translation at the 5' end of the template. If translation of the sgRNA is similar to the gRNA, then the negative effect of a resident PTE on translation should have been discernable in assays with ΔK and ΔKΔT. Instead, ΔK and ΔKΔT reduced translation of p26 and p27 by a similar amount as ΔKΔPΔT or Δ3'UTR using full-length sgRNA transcripts *in vitro*, and *in vivo* using p26-LUC and p27-LUC (Fig. 3). In addition, in the absence of a PTE *in cis*, translation of p26 and p27 from sgRNA ΔKΔPΔT was less affected by the presence of PTE *in trans* 2.6–3-fold reduction) compared with similar assays conducted for the gRNA (5-fold reduction) (Du et al., 2017). This suggests that 3'CITE-independent translation of the gRNA is more dependent on limiting amounts of eIF4F, and supports the existence of different translation requirements for PEMV2 gRNA and sgRNA. Different translation mechanisms utilized by gRNA and sgRNA were also reported for *Tobacco mosaic virus* U1, where translation of the gRNA is cap-dependent and translation of the uncapped I_2 sgRNA requires an IRES at its 5' end (Joshi et al., 1983; Skulachev et al., 1999). Such distinctive translation mechanisms may reflect a regulatory strategy to fine-tune the patterns of viral protein expression at various stages of viral life cycle.

3.3. Translation of p26 and p27 may not use canonical leaky scanning

Translation initiation at AUG^{26} and AUG^{27} appears to be competitive as elimination of either AUG^{26} and AUG^{27} increased translation at the other initiation codon *in vitro* and *in vivo* (Fig. 2C, D). In addition, mutations in AUG^{27} enhanced accumulation of the gRNA by 1.7-fold (Fig. 1E), possibly due to augmented synthesis of p26, which is required for gRNA accumulation (Fig. 1E). These results do not appear to be consistent with a canonical leaky scanning mode of translation, in which initiation is a 5'-dependent sequential process with no coupling or competition between the two initiation AUGs. Our results are similar to the translation initiation behavior of two closely-spaced AUG initiation codons in *Turnip yellow mosaic virus* (TYMV). Cap-dependent translation of the overlapping ORFs for p69 and p206 proceeds after ribosome scanning through the 87-nt 5'UTR to initiation codons separated by 7 nt using a mechanism that is regulated by the proximity of the two initiation codons (Matsuda and Dreher, 2006). This proximity modifies canonical leaky scanning such that initiation decisions at the two start codons are no longer strictly sequential with 5'-polarity, but rather competitive. Gradual separation of the closely spaced initiation codons eliminated the competition, changing the transcripts from dicistronic to monocistronic. The authors proposed a "backward scanning" model in which the net movement of scanning ribosomes from 5' to 3' involves forward and backward oscillations covering a range of 15 nt (Matsuda and Dreher, 2006). Unlike TYMV, PEMV2 sgRNA is uncapped with only a 9-nt 5'UTR and there is also a greater distance between the two initiation codons. We are currently investigating whether similar oscillations are responsible for competitive translation of AUG^{26} and AUG^{27}.

4. Material and methods

4.1. Mapping the sgRNA 5' end

The 5'-end of PEMV2 sgRNA was mapped by primer extension using Superscript III reverse transcriptase, as described previously (Wang and Simon, 1997). Briefly, 1 μg of total RNA isolated from PEMV2-infected protoplasts at 24 hpi was annealed to 0.5 pmol of 5'-end-[γ-^{32}P] ATP-labeled primer complementary to PEMV2 positions 2845–2869. Superscript III reverse transcriptase (25 U, Invitrogen) was added and the reaction allowed to proceed at 52 °C for 60 min. Total RNA extracted from protoplasts transfected with a replication-incompetent mutant (PEMV2 GDD) served as a negative control. Samples were resolved on 8% denaturing acrylamide gels. The gel was dried and exposed to a phosphorimager screen, which was subsequently scanned by a FLA-5100 fluorescent image analyzer (Fujifilm).

4.2. Plasmid construction

Full length PEMV2 sgRNA was PCR amplified using a T7 promotor-containing forward primer incorporating an *Eco*RI restriction site and a reverse primer with a *Sma*I restriction site. The resulting PCR products were gel purified and cloned into pUC19 using *Eco*RI and *Sma*I to generate pUC19-sgRNA. Desired mutations were introduced using custom-designed oligonucleotide primers (Integrated DNA Technologies) using Quick-change one-step site-directed mutagenesis (Liu and Naismith, 2008). PCR products were cloned into pUC19-sgRNA to replace the corresponding fragment. Luciferase reporter constructs p26-LUC and p27-LUC contained the sgRNA 5'UTR and initial 49 codons of the p26 ORF or 44 codons of the p27 ORF fused to the firefly luciferase ORF and then the PEMV2 full-length 3'UTR. Sequences of all constructs were confirmed (Eurofins Genomics).

4.3. In vitro RNA transcription and translation

RNA transcripts were transcribed *in vitro* using bacteriophage T7 RNA polymerase. pUC19-sgRNA constructs or luciferase reporter constructs were linearized with *Sma*I or *Ssp*I, respectively, to serve as DNA templates for RNA transcription. For *in vitro* translation, 10 μl translation mixtures contained 5 μl WGE (Promega), 0.5 pmol RNA template, 0.8 μl of 1 mM amino acids mix (Met^-), 100 mM potassium acetate and 0.5 μl [5μCi] ^{35}S-methionine. The translation mixture was incubated at 25 °C for 45 min and then resolved on a 10% SDS-PAGE gel. The gel was dried and exposed to a phosphorimager screen, which was subsequently scanned by a FLA-5100 fluorescent image analyzer (Fujifilm). The intensity of radioactive bands was quantified using Multi Gauge Ver. 2.0 (Fujifilm).

4.4. Ribosome toeprinting

Translation reactions were as described above except that complete amino acids mixtures were used, ^{35}S-methionine was omitted, and 1 mM CHX was supplied and the reaction incubated at 25 °C for 45 min. The translation reaction (3.5 μl) was then mixed with 5 μl of primer annealing buffer (1x Superscript III reverse transcriptase buffer, 10 mM DTT, 0.5 mM dNTPs, 1 mM CHX and 1 U/μl RNaseout ribonuclease inhibitor)

and incubated at 55 °C for 2 min. The [γ-^{32}P] ATP-labeled primer (1 pmol), which was complementary to PEMV2 positions 2875–2898, was added and incubation continued at 37 °C for 5 min. Superscript III reverse transcriptase (25 U, Invitrogen) was then added and primers extended at 37 °C for 30 min. Samples were resolved on a 8% denaturing acrylamide gel. The gel was dried and exposed to a phosphorimager screen as described above.

4.5. SHAPE structure probing

SHAPE structure probing was performed as previously described (Wilkinson et al., 2006). PEMV2 sgRNA was *in vitro* transcribed and purified by phenol-chloroform extraction and ethanol precipitation. The resulting RNA was denatured at 65 °C before subjection to folding in SHAPE folding buffer (80 mM Tris-Cl, [pH 8.0], 11 mM $Mg(CH_3COO)_2$, 160 mM NH_4Cl) at 37 °C for 20 min. Folded RNA was treated with either 15 mM N-methylisatoic anhydride (NMIA) or with the same volume of dimethyl sulfoxide (DMSO). A [γ-^{32}P] ATP-labeled oligonucleotide complementary to PEMV2 positions 2908–2933 was used for primer extension reactions. The resulting cDNA products along with ladders generated by Sanger sequencing were resolved on 8% urea-based polyacrylamide gels. Gels were then dried and exposed to a phosphorimager screen as described above. RNA secondary structures were generated by combining structure probing results and the best-fitting Mfold prediction (Zuker, 2003).

4.6. Protoplast transfection, Northern blots and in vivo luciferase assays

Arabidopsis thaliana protoplasts were prepared from callus cultures and transfected using a polyethylene glycol-mediated transformation protocol as previously described (Gao et al., 2012). Briefly, 5 ×10^6 protoplasts were transfected with 20 μg of PEMV2 gRNA or luciferase reporter transcripts. Cells were collected for RNA extraction at 24 hpi for gRNA-infected samples or were lysed at 18 hpi for luciferase reporter transfected samples. Total RNA was prepared using RNA extraction buffer (50 mM Tris-HCl [pH 7.5], 5 mM EDTA [pH 8.0], 100 mM NaCl, 1% SDS), followed by phenol-chloroform extraction and ethanol precipitation. Thermally denatured RNAs were subjected to electrophoresis through 1% agarose gels, transferred to nitrocellulose and probed with [γ-^{32}P] ATP-labeled oligonucleotides complementary to PEMV2 positions 3229–3270, 2969–3004, and 2731–2771. Blots were exposed to a phosphorimager screen as described above. For luciferase assays, luciferase activity in protoplasts was assayed with a Dual-Luciferase® Reporter Assay System (Promega) using Modulus microplate multimode reader (Turner BioSystems).

4.7. Statistical analysis

Data from three independent experiments were statistically analyzed using ANOVA or *t*-test as indicated (Graphpad prism 7.0).

Acknowledgements

We thank Zhiyou Du for helpful discussions. This work was supported by the National Science Foundation (MCB-1411836) and National Institutes of Health (R21AI117882-01) to A.E.S. F. G. was supported by National Institutes of Health Ruth Kirschstein Award T32AI125186A.

References

Adams, M.J., Lefkowitz, E.J., King, A.M.Q., Bamford, D.H., Breitbart, M., Davison, A.J., Ghabrial, S.A., Gorbalenya, A.E., Knowles, N.J., Krell, P., Lavigne, R., Prangishvili, D., Sanfacon, H., Siddell, S.G., Simmonds, P., Carstens, E.B., 2015. Ratification vote on taxonomic proposals to the International Committee on Taxonomy of Viruses (2015). Arch. Virol. 160, 1837–1850.

Aitken, C.E., Lorsch, J.R., 2012. A mechanistic overview of translation initiation in eukaryotes. Nat. Struct. Mol. Biol. 19, 568–576.

Battiste, J.L., Pestova, T.V., Hellen, C.U.T., Wagner, G., 2000. The eIF1A solution structure reveals a large RNA-binding surface important for scanning function. Mol. Cell 5, 109–119.

Chattopadhyay, M., Kuhlmann, M.M., Kumar, K., Simon, A.E., 2014. Position of the kissing-loop interaction associated with PTE-type 3'CITEs can affect enhancement of cap-independent translation. Virology 458, 43–52.

Chattopadhyay, M., Shi, K., Yuan, X., Simon, A.E., 2011. Long-distance kissing loop interactions between a 3 ' proximal Y-shaped structure and apical loops of 5 ' hairpins enhance translation of Saguaro cactus virus. Virology 417, 113–125.

Chkuaseli, T., Newburn, L.R., Bakhshinyan, D., White, K.A., 2015. Protein expression strategies in Tobacco necrosis virus-D. Virology 486, 54–62.

Das, R., Laederach, A., Pearlman, S.M., Herschlag, D., Altman, R.B., 2005. SAFA: semi-automated footprinting analysis software for high-throughput quantification of nucleic acid footprinting experiments. RNA 11, 344–354.

Das Sharma, S., Kraft, J.J., Miller, W.A., Goss, D.J., 2015. Recruitment of the 40S ribosomal subunit to the 3 '-untranslated region (UTR) of a viral mRNA, via the eIF4 complex, facilitates cap-independent translation. J. Biol. Chem. 290, 11268–11281.

Demler, S.A., Rucker, D.G., Dezoeten, G.A., 1993. The chimeric nature of the genome of Pea enation mosaic virus- The independent replication of RNA-2. J. Gen. Virol. 74, 1–14.

Du, Z., Alekhina, O.M., Vassilenko, K.S., Simon, A.E., 2017. Concerted action of two 3' cap-independent translation enhancers increases the competitive strength of translated viral genomes. Nucleic Acids Res., (in press).

Fabian, M.R., White, K.A., 2004. 5'–3' RNA-RNA interaction facilitates cap- and poly(A) tail-independent translation of tomato bushy stunt virus mRNA - A potential common mechanism for Tombusviridae. J. Biol. Chem. 279, 28862–28872.

Fabian, M.R., White, K.A., 2006. Analysis of a 3'-translation enhancer in a tombusvirus: a dynamic model for RNA-RNA interactions of mRNA termini. RNA 12, 1304–1314.

Firth, A.E., Brierley, I., 2012. Non-canonical translation in RNA viruses. J. Gen. Virol. 93, 1385–1409.

Gao, F., Gulay, S.P., Kasprzak, W., Dinman, J.D., Shapiro, B.A., Simon, A.E., 2013. The kissing-loop T-shaped structure translational enhancer of Pea enation mosaic virus can bind simultaneously to ribosomes and a 5 ' proximal hairpin. J. Virol. 87, 11987–12002.

Gao, F., Kasprzak, W., Stupina, V.A., Shapiro, B.A., Simon, A.E., 2012. A ribosome-binding, 3 ' translational enhancer has a T-shaped structure and engages in a long-distance RNA-RNA interaction. J. Virol. 86, 9828–9842.

Gao, F., Kasprzak, W.K., Szarko, C., Shapiro, B.A., Simon, A.E., 2014. The 3 ' untranslated region of Pea enation mosaic virus contains two T-shaped, ribosome-binding, cap-independent translation enhancers. J. Virol. 89, 11696–11712.

Gao, F., Simon, A.E., 2016. Multiple cis-acting elements modulate programmed-1 ribosomal frameshifting in Pea enation mosaic virus. Nucleic Acids Res. 44, 878–895.

Gazo, B.M., Murphy, P., Gatchel, J.R., Browning, K.S., 2004. A novel interaction of cap-binding protein complexes eukaryotic initiation factor (eIF) 4F and eIF(iso)4F with a region in the 3 '-untranslated region of satellite tobacco necrosis virus. J. Biol. Chem. 279, 13584–13592.

Gowda, S., Ayllon, M.A., Satyanarayana, T., Bar-Joseph, M., Dawson, W.O., 2003. Transcription strategy in a Closterovirus: a novel 5 '-proximal controller element of Citrus tristeza virus produces 5 '- and 3 '-terminal subgenomic RNAs and differs from 3 ' open reading frame controller elements. J. Virol. 77, 340–352.

Guan, H.C., Carpenter, C.D., Simon, A.E., 2000. Analysis of cis-acting sequences involved in plus-strand synthesis of a turnip crinkle virus-associated satellite RNA identifies a new carmovirus replication element. Virology 268, 345–354.

Guo, L., Allen, E.M., Miller, W.A., 2001. Base-pairing between untranslated regions facilitates translation of uncapped, nonpolyadenylated viral RNA. Mol. Cell 7, 1103–1109.

Hecht, A., Glasgow, J., Jaschke, P.R., Bawazer, L.A., Munson, M.S., Cochran, J.R., Endy, D., Salit, M., 2017. Measurements of translation initiation from all 64 codons in E. coli. Nucleic Acids Res. 45, 3615–3626.

Jackson, R.J., Hellen, C.U.T., Pestova, T.V., 2010. The mechanism of eukaryotic translation initiation and principles of its regulation. Nat. Rev. Mol. Cell Biol. 11, 113–127.

Joshi, S., Pleij, C.W.A., Haenni, A.L., Chapeville, F., Bosch, L., 1983. Properties of the Tobacco mosaic virus intermediate length RNA-2 and its translation. Virology 127, 100–111.

Kim, S.H., MacFarlane, S., Kalinina, N.O., Rakitina, D.V., Ryabov, E.V., Gillespie, T., Haupt, S., Brown, J.W.S., Taliansky, M., 2007a. Interaction of a plant virus-encoded protein with the major nucleolar protein fibrillarin is required for systemic virus infection. Proc. Natl. Acad. Sci. USA 104, 11115–11120.

Kim, S.H., Ryabov, E.V., Kalinina, N.O., Rakitina, D.V., Gillespie, T., MacFarlane, S., Haupt, S., Brown, J.W.S., Taliansky, M., 2007b. Cajal bodies and the nucleolus are required for a plant virus systemic infection. EMBO J. 26, 2169–2179.

Kozak, M., 1999. Initiation of translation in prokaryotes and eukaryotes. Gene 234, 187–208.

Liu, H., Naismith, J.H., 2008. An efficient one-step site-directed deletion, insertion, single and multiple-site plasmid mutagenesis protocol. BMC Biotech. 8, 91.

Matsuda, D., Dreher, T.W., 2006. Close spacing of AUG initiation codons confers dicistronic character on a eukaryotic mRNA. RNA 12, 1338–1349.

McCormack, J.C., Yuan, X., Yingling, Y.G., Kasprzak, W., Zamora, R.E., Shapiro, B.A., Simon, A.E., 2008. Structural domains within the 3' untranslated region of Turnip crinkle virus. J. Virol. 82, 8706–8720.

Miras, M., Miller, W.A., Truniger, V., Aranda, M.A., 2017. Non-canonical translation in plant RNA viruses. Front. Plant Sci. 8, 494.

Miras, M., Sempere, R.N., Kraft, J.J., Miller, W.A., Aranda, M.A., Truniger, V., 2014. Interfamilial recombination between viruses led to acquisition of a novel translation-enhancing RNA element that allows resistance breaking. New Phytol. 202, 233–246.

Nicholson, B.L., White, K.A., 2008. Context-influenced cap-independent translation of Tombusvirus mRNAs in vitro. Virology 380, 203–212.
Nicholson, B.L., White, K.A., 2011. 3' Cap-independent translation enhancers of positive-strand RNA plant viruses. Curr. Opin. Virol. 1, 373–380.
Nicholson, B.L., Wu, B., Chevtchenko, I., White, K.A., 2010. Tombusvirus recruitment of host translational machinery via the 3' UTR. RNA 16, 1402–1419.
Nicholson, B.L., Zaslaver, O., Mayberry, L.K., Browning, K.S., White, K.A., 2013. Tombusvirus Y-shaped translational enhancer forms a complex with eIF4F and can be functionally replaced by heterologous translational enhancers. J. Virol. 87, 1872–1883.
Pisareva, V.P., Pisarev, A.V., Komar, A.A., Hellen, C.U.T., Pestova, T.V., 2008. Translation initiation on mammalian mRNAs with structured 5' UTRs requires DExH-Box protein DHX29. Cell 135, 1237–1250.
Rakotondrafara, A.M., Polacek, C., Harris, E., Miller, W.A., 2006. Oscillating kissing stem-loop interactions mediate 5' scanning-dependent translation by a viral 3'-cap-independent translation element. RNA 12, 1893–1906.
Ryabov, E.V., Oparka, K.J., Santa Cruz, S., Robinson, D.J., Taliansky, M.E., 1998. Intracellular location of two groundnut rosette umbravirus proteins delivered by PVX and TMV vectors. Virology 242, 303–313.
Ryabov, E.V., Roberts, I.M., Palukaitis, P., Taliansky, M., 1999. Host-specific cell-to-cell and long-distance movements of cucumber mosaic virus are facilitated by the movement protein of groundnut rosette virus. Virology 260, 98–108.
Ryabov, E.V., Robinson, D.J., Taliansky, M., 2001. Umbravirus-encoded proteins both stabilize heterologous viral RNA and mediate its systemic movement in some plant species. Virology 288, 391–400.
Sarawaneeyaruk, S., Iwakawa, H., Mizumoto, H., Murakami, H., Kaido, M., Mise, K., Okuno, T., 2009. Host-dependent roles of the viral 5' untranslated region (UTR) in RNA stabilization and cap-independent translational enhancement mediated by the 3' UTR of Red clover necrotic mosaic virus RNA1. Virology 391, 107–118.
Shen, R., Rakotondrafara, A.M., Miller, W.A., 2006. Trans regulation of cap-independent translation by a viral subgenomic RNA. J. Virol. 80, 10045–10054.
Simon, A.E., Miller, W.A., 2013. 3 ' Cap-independent translation enhancers of plant viruses. Ann. Rev. Microbiol. 67, 21–42.
Skulachev, M.V., Ivanov, P.A., Karpova, O.V., Korpela, T., Rodionova, N.P., Dorokhov, Y.L., Atabekov, J.G., 1999. Internal initiation of translation directed by the 5 '-untranslated region of the tobamovirus subgenomic RNA I-2. Virology 263, 139–154.
Stupina, V.A., Meskauskas, A., McCormack, J.C., Yingling, Y.G., Shapiro, B.A., Dinman, J.D., Simon, A.E., 2008. The 3' proximal translational enhancer of Turnip crinkle virus binds to 60S ribosomal subunits. RNA 14, 2379–2393.
Sztuba-Solinska, J., Stollar, V., Bujarski, J.J., 2011. Subgenomic messenger RNAs: mastering regulation of (+)-strand RNA virus life cycle. Virology 412, 245–255.
Taliansky, M., Roberts, I.M., Kalinina, N., Ryabov, E.V., Raj, S.K., Robinson, D.J., Oparka, K.J., 2003. An umbraviral protein, involved in long-distance RNA movement, binds viral RNA and forms unique, protective ribonucleoprotein complexes. J. Virol. 77, 3031–3040.
Tatineni, S., Afunian, M.R., Gowda, S., Hilf, M.E., Bar-Joseph, M., Dawson, W.O., 2009. Characterization of the 5 '- and 3 '-terminal subgenomic RNAs produced by a capillovirus: evidence for a CP subgenomic RNA. Virology 385, 521–528.
Thiebeauld, O., Pooggin, M., Ryabova, L., 2007. Alternative translation strategies in plant viruses. Plant Virus. 1, 20.
Treder, K., Kneller, E.L.P., Allen, E.M., Wang, Z.H., Browning, K.S., Miller, W.A., 2008. The 3' cap-independent translation element of barley yellow dwarf virus binds eIF4F via the eIF4G subunit to initiate translation. RNA 14, 134–147.
Valverde, R.A., Sabanadzovic, S., 2009. A novel plant virus with unique properties infecting Japanese holly fern. J. Gen. Virol. 90, 2542–2549.
Vives, M.C., Galipienso, L., Navarro, L., Moreno, P., Guerri, J., 2002. Characterization of two kinds of subgenomic RNAs produced by citrus leaf blotch virus. Virology 295, 328–336.
Wang, J.L., Simon, A.E., 1997. Analysis of the two subgenomic RNA promoters for turnip crinkle virus in vivo and in vitro. Virology 232, 174–186.
Wang, Z., Treder, K., Miller, W.A., 2009. Structure of a viral cap-independent translation element that functions via high affinity binding to the eIF4E subunit of eIF4F. J. Biol. Chem. 284, 14189–14202.
Wilkinson, K.A., Merino, E.J., Weeks, K.M., 2006. Selective 2 '-hydroxyl acylation analyzed by primer extension (SHAPE): quantitative RNA structure analysis at single nucleotide resolution. Nat. Protoc. 1, 1610–1616.
Wu, B., Pogany, J., Na, H., Nicholson, B.L., Nagy, P.D., White, K.A., 2009. A discontinuous RNA platform mediates RNA virus replication: building an integrated model for RNA-based regulation of viral processes. PLoS Pathog. 5, e1000323.
Wu, B.D., Oliveri, S., Mandic, J., White, K.A., 2010. Evidence for a premature termination mechanism of subgenomic mRNA transcription in a carmovirus. J. Virol. 84, 7904–7907.
Zaccomer, B., Haenni, A.L., Macaya, G., 1995. The remarkable variety of plant RNA virus genomes. J. Gen. Virol. 76, 231–247.
Zuker, M., 2003. Mfold web server for nucleic acid folding and hybridization prediction. Nucleic Acids Res. 31, 3406–3415.